

Differential Evolution Algorithm Based Very Fast Renewable Energy System Optimisation Tool Design

Cemil Altin

*Department of Electrical and Electronics Engineering, Yozgat Bozok University,
Adnan Menderes Bulvari, Ataturk Yolu 7. Km D:118, 66200 Merkez/Yozgat, Turkey
cemil.altin@yobu.edu.tr*

Abstract—In this study, an optimisation tool that uses the differential evolution algorithm with a special distribution strategy is designed for the first time to be used in the optimisation of hybrid renewable energy systems. The developed tool and the hybrid optimisation model for multiple energy resources (HOMER) optimisation programme were compared. The tool is much faster than the HOMER programme and can produce almost the same results as HOMER. In addition, a heuristic-based optimisation technique was used for the first time to generate extremely comprehensive findings. The capacity shortage parameter, which is not used much in the literature, is used as a reliability parameter. The cost of energy (COE) was used as the cost function. The results are promising for detailed optimisation studies in this area.

Index Terms—Differential evolution; HOMER; Hybrid; Optimisation.

I. INTRODUCTION

In this study, optimisation processes were carried out using the differential evolution (DE) algorithm. The DE algorithm is an optimisation algorithm developed by Storn and Price [1]. With the DE algorithm, the dimensions of the photovoltaic panel PV, wind turbine, battery and inverter components and the wind speed parameters are simultaneously optimised for the most optimal system. The cost of energy (COE) parameter served as a cost function during the optimisation phase. The reliability parameter was the capacity shortage parameter. Systems that are below the maximum permitted capacity shortage are regarded reliable systems in the optimisation problem. The capacity shortage parameter is used to build a trustworthy system and ensure that it generates the required amount of energy. In the hybrid optimisation model for multiple energy resources (HOMER) programme, the capacity shortage is also employed as a system reliability metric. COE, levelized energy cost (LCOE), total annual cost (TAC), and total cost (TC) parameters have been used by many researchers as cost functions. As a reliability parameter, many researchers prefer the loss of power supply probability (LPSP) parameter. However, the LPSP option might cause the system to be undersized and unresponsive, particularly during sudden surges in load. In this sense, optimisation that

takes into account capacity shortage is more favourable and results in more precise system sizing. Because a percentage of the production is set aside for unplanned loads and adequate energy is assumed to satisfy the predefined additional instant loads during the simulation process to establish the capacity shortage. The studies in the literature on this topic are given in Table I below.

TABLE I. WORKS IN THE LITERATURE AND THE METHODS THEY USE.

Algorithm	Hybrid System (HRES)	Cost Function	Reliability Parameter	Ref.
Grey Wolf	PV-WT-BM	LCOE	LPSP	[2]
	PW-WT	ACS	LPSP	[3]
Ant Colony	PV-WT-BAT-HY	TAC	LPSP	[4]
Genetic Algorithm	PV-WT-BAT	COE	LPSP	[5]
	PV-WT-BAT	COE	LPSP	[6]
Flower Pollination	PV-FC	TAC	LPSP	[7]
Social Spider Optimiser	PV-WT-DG	COE	LPSP	[8]
Equilibrium Optimiser	PV-WT-BAT-DG	NPC	LPSP	[9]
	PV-PS	NPC	LPSP	[10]
Multimodal Delayed PSO	PV-WT-BAT-DG	LCOE	LPSP	[11]
Linear Programming	PV-BAT	TC	LPSP	[12]
MPSO/GA	PV-WT-BAT	TNPC	LPSP	[13]
Dragon Fly	PV-WT-FC	NPC	LPSP	[14]
Water Strider	PV-FC	TAC	LPSP	[15]
Multi Objective Crow Search Algorithm	PV-FC-DG	TNPC	LPSP	[16]
Dynamic Programming	PV-WT-BAT-DG	LCC	---	[17]
Runge Kutta	PV-BM-BAT	COE	LPSP	[18]
Artificial Bee Colony	PV-WT-FC	TAC	LPSP	[19]
	PV-WT-BAT	TAC	LPSP	[20]
Differential Evolution	PV-WT-BAT-INV PV-BAT-INV WT-BAT-INV	COE	Capacity Shortage	This Work

Tezer, Yaman, and Yaman [21] provide comprehensive details on the cost functions and reliability metrics used in the literature [21]. Reliability is determined by the LPSP reliability parameter by adding the instances in which the load cannot be fully fed and dividing by the whole amount of time (8760 hours). However, it is unknown how much of the load is not fed when it is not fed. Since this study prefers the capacity shortage parameter over the LPSP parameter. How much of the load is not fed matters in the capacity shortage parameter when the load cannot be fed entirely. In

this regard, the study is different from studies in the literature.

II. OPTIMISATION

The differential evolution (DE) algorithm was used in this optimisation process (Storn and Price, 1995). DE is a new parallel direct search method that uses parameter vectors for each generation (G) of N_p members. The generation population does not change during the optimisation process. If nothing is known about the system, the initial population is chosen at random. As a rule, a uniform probability distribution is assumed for all random decisions, unless otherwise stated. If a preliminary solution is available, the initial population is usually formed by adding normally distributed random deviations to the nominal solution. DE generates new parameter vectors by adding the weighted difference vector between two population members to a third member. If the resulting vector yields a lower objective function value than a predetermined population member, the newly generated vector replaces the vector with which it was compared. In addition, the best parameter vector is evaluated for each generation of G to track progress in the optimisation process. Extraction of distance and direction information from the population to generate random deviations is done by an adaptive algorithm with excellent convergence properties. The DE algorithm uses a cost function for optimisation. In this study, the cost function is the cost of energy (COE) according to the reliability parameter. It is the minimum cost per kWh. Its unit is \$/kWh. The COE value is calculated by providing the reliability parameter. The user sets the value of the reliability parameter to feed the load. Electrical reliability systems are those that meet the reliability parameter. Systems that can electrically feed the load are reliable systems. In contrast to the research in the literature, the capacity shortage parameter in this study is the reliability parameter. The loss of power supply probability (LPSP) parameter has been used in numerous research throughout the literature, as can be seen in Table I:

$$LPSP = \frac{\sum_{t=1}^{8760} \text{Time}(\text{if } E_{\text{avail}}(t) < E_{\text{load}}(t))}{8760}, \quad (1)$$

$$E_{\text{avail}}(t) = E_{\text{pv}}(t) + E_{\text{wind}}(t) + E_{\text{bat}}(t). \quad (2)$$

Because it is simple to use, this parameter is commonly used in the optimisation of hybrid renewable energy systems. The LPSP parameter has two drawbacks, being a system reliability criterion. The first of these drawbacks is the instantaneous feeding of the load in the LPSP parameter. The load is seen as fed if it can be fed entirely and is regarded as unfed if it cannot. In other words, the hybrid system is considered to be fed if it produces 100 kW or more in an instant for a load of 100 kW. However, it is not considered to be fed if even a small portion of it cannot be fed. In other words, even if the hybrid system produces 99.9 kW momentarily, it means that the system cannot be fed. Therefore, it does not matter how much of the load cannot be fed. So, it is clear that this will not be true in sensitive designs. The operating reserve is not included, which is the second drawback of the LPSP parameter. As a

result, the system does not have the capacity to handle potential increases in load and its reliability is limited. However, how much of the load is fed or not is considered in the capacity shortage parameter. Additionally, additional loads are supported by the energy that has been reserved. For reliable systems, the COE value is determined during optimisation, and for unstable systems, the COE is accepted as infinite, enabling the algorithm to skip these systems. The flow diagram of the DE algorithm used for hybrid renewable energy resource optimisation is given in Fig. 1 below.

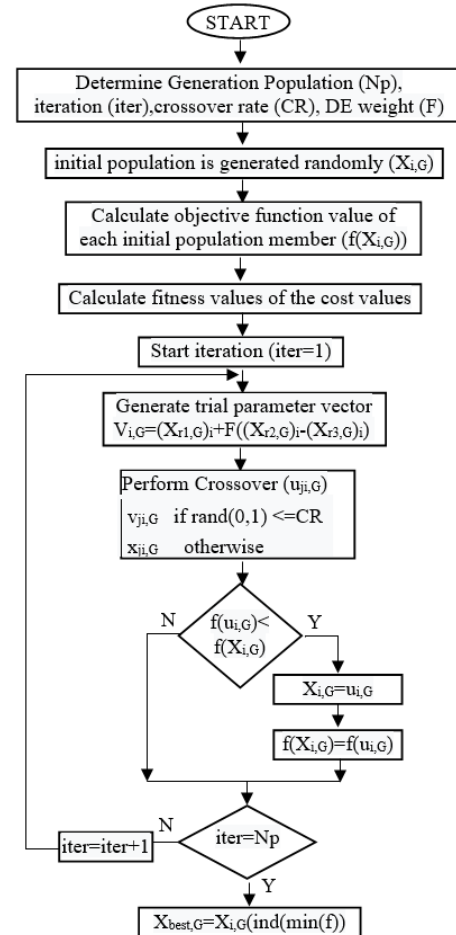


Fig. 1. DE algorithm flow chart.

In the DE algorithm, it produces new parameter vectors by adding the weighted difference vector between two population members to a third member. How this is done is shown in Fig. 2 below.

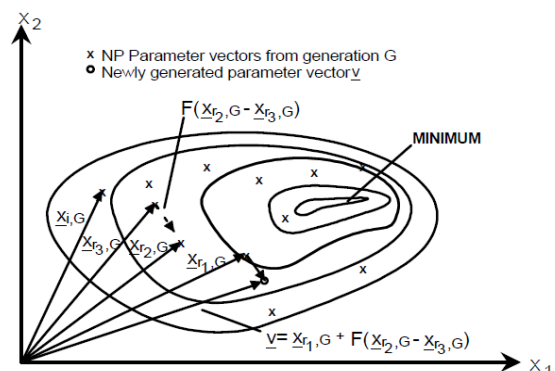
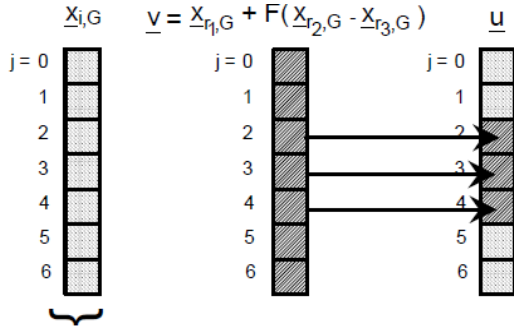


Fig. 2. Generation of new parameter vectors by adding the weighted difference vector between two members of the population to a third member [1].

Figure 3 shows how the crossover operation is performed in the DE algorithm.



Parameter vector containing the parameters x_i , $j=0, 1, \dots, D-1$

Fig. 3. Crossover process [1].

The parameters of the differential evolution algorithm that need to be adjusted during the optimisation process and the values preferred in this study are presented in Table II.

TABLE II. PARAMETERS OF THE DIFFERENTIAL EVOLUTION ALGORITHM.

Parameters	Values
Number of population (N_p)	15
Iteration (iter)	100
Crossover rate (CR)	0.8
DE weight (F)	0.8

III. DISPATCH STRATEGY

The control of energy flows between the elements of the hybrid renewable energy source system is handled by the dispatch strategy. It is a set of laws that govern how electrical energy generated from renewable sources is transferred to the battery, the load or the energy stored in the battery is transferred to the load to feed the load. Figure 4 illustrates the process flow for the dispatch approach. Knowing the net energy that can be pulled from the battery group is essential for the dispatch plan (after the losses are subtracted). The energy stored in the battery, as well as the energy generated by the solar panels and wind turbine, will be used to power the load. The following equations are used to determine the net energy that can be extracted from the battery group:

$$E_{\text{bat}} = N_{\text{bat}} \times V_{\text{nom}} \times Q_{\text{max}}, \quad (3)$$

$$E_{\text{min}} = \text{SOC}_{\text{min}} \times E_{\text{bat}}, \quad (4)$$

$$\eta_{\text{bat}} = \sqrt{\eta_{\text{rt}}}, \quad (5)$$

$$E_{\text{net}} = (E_{\text{bat}} - E_{\text{min}}) \times \eta_{\text{bat}}. \quad (6)$$

Here, SOC is the state of charge, Q_{max} is the maximum capacity of the battery, and η_{rt} is the roundtrip efficiency of the battery. After that, the whole amount of production and complete amount of consumption are taken into account to determine the charge or discharge energy:

$$E_{\text{available}} = E_{\text{PV}} + E_{\text{wind}} + E_{\text{net}}, \quad (7)$$

$$E_{\text{consumption}} = E_{\text{load}} + E_{\text{inv_loss}} + E_{\text{char_dischar_loss}}, \quad (8)$$

$$E_{\text{char,dischar}} = E_{\text{available}} - E_{\text{consumption}}. \quad (9)$$

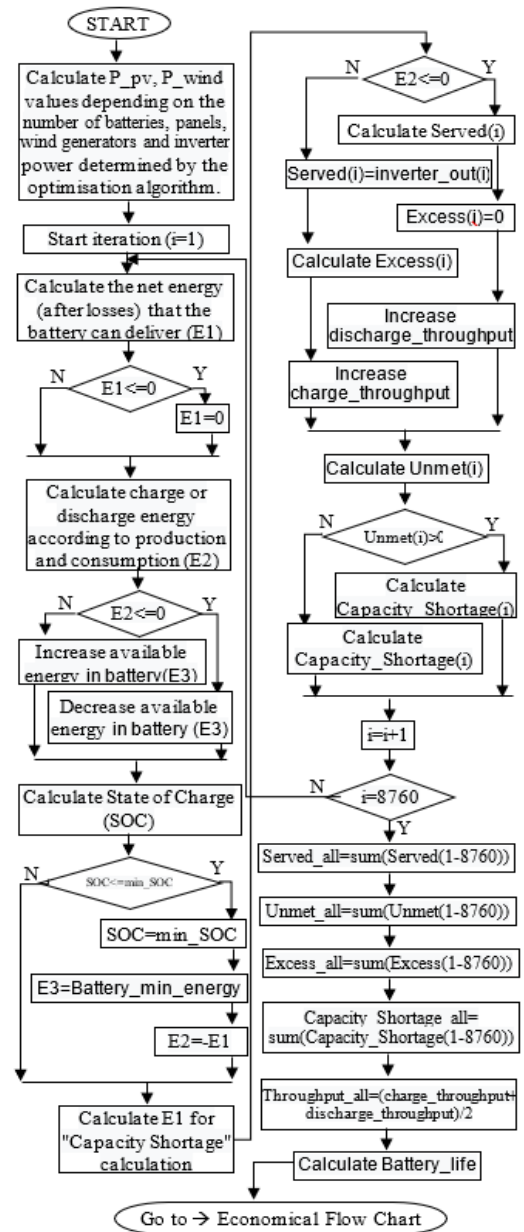


Fig. 4. Dispatch strategy flow chart.

It is necessary to charge the battery pack if $E_{\text{char,dischar}_i} \geq 0$. However, some limitations apply to the amount of energy that the battery may take in or expend during charging and discharging. In other words, the battery group may not always be able to absorb all of the extra energy left after the load is supplied for charging purposes. Similarly, all the energy needed to temporarily power the load cannot be drawn from the battery group when the energy generated by the panel and the wind turbine is inadequate. As a result, the maximum charge and discharge power capacity of the battery pack is determined hourly. This is another originality of this work. No description of the regulations that govern battery charging and discharging was provided in earlier studies. However, in hybrid system designs, the battery charge and discharge technique is of essential importance. Depending on the state of charge of the battery pack, the maximum charging power fluctuates hourly. The maximum charging power is calculated using three different techniques. These methods are the Kinetic

Battery Model [22], maximum charge rate, and maximum battery charge current. The lowest quantity among these three is taken as the maximum charging power of the battery pack once these three values have been calculated. The following describes how the three parameters are calculated:

$$P_{k_{bm,d}} = \frac{-kcQ_{max} + kQ_1 e^{-k\Delta t} + Qkc(1 - e^{-k\Delta t})}{1 - e^{-k\Delta t} + c(k\Delta t - 1 + e^{-k\Delta t})}, \quad (10)$$

$$P_{m_{cr}} = \frac{(1 - e^{-a_c \Delta t})(Q_{max} - Q)}{\Delta t}, \quad (11)$$

$$P_{m_{cc}} = \frac{N_{bat} I_{max} V_{nom}}{1000}. \quad (12)$$

After subtracting charge losses from the smallest of these three estimated values, the maximum charge power is calculated as shown below

$$P_{max,c} = \frac{\text{MIN}(P_{k_{bm,d}}, P_{m_{cr}}, P_{m_{cc}})}{\eta_{bat,c}}. \quad (13)$$

The discharge process follows a set of rules, much like the charging process. It is established how much electricity the battery pack can produce at its highest rate per hour. The kinetic battery model computes this parameter, which is denoted as the maximum discharge power

$$P_{k_{bm,c}} = \frac{kQ_1 e^{-k\Delta t} + Qkc(1 - e^{-k\Delta t})}{1 - e^{-k\Delta t} + c(k\Delta t - 1 + e^{-k\Delta t})}. \quad (14)$$

Following the elimination of the discharge losses, the maximum discharge power is calculated

$$P_{max,d} = \eta_{bat,d} P_{k_{bm,d}}. \quad (15)$$

The state of charge (SOC) must be determined after charging or discharging to be used in later steps or cycles. The minimum SOC value of the batteries used is $SOC_{min} = 0.3$, i.e., 30%. The SOC is calculated as follows

$$SOC = \frac{E_{bat_after_c,d}}{N_{bat} \times V_{nom} \times Q_{max}}. \quad (16)$$

Following these actions, the hourly total energy production and consumption values are used to calculate other parameters of the hybrid energy system. These parameters are served energy, excess energy, unmet energy, and most importantly, the capacity shortage parameter, which is the reliability parameter obtained through these calculations.

It would be helpful to remind everyone that converter optimisation was also carried out in this study before moving on to the calculation of these parameters. A converter is a device that transforms energy, whether it is DC energy from sources like PV and batteries into AC energy for AC loads or AC energy into DC energy from sources like wind turbines and generators for battery charging or DC loads. The converter element (inverter + rectifier) experiences losses during the conversion of DC to AC (inverter) or AC to DC (rectifier). Therefore, it is

important to consider these losses in simulations and design. Energy costs can be reduced by carefully choosing the converter power in hybrid system designs. Inverter power should not be less than the power needed to feed the necessary number of loads pulled throughout the year, nor should it be greater than the peak drawn power throughout the year. The energy served is equivalent to the load power for powers lower than the inverter power. The energy served for powers more than the inverter power is equal to the inverter power, and the extra energy is regarded as unmet energy.

Following this knowledge, the equations below show how the aforementioned parameters were each determined. First of all, when speaking of the served energy, it should be understood that this refers to the total amount of energy that can be provided to the loads throughout the year (8760 hours)

$$E_{served} = \begin{cases} E_{load}, & \text{if } E_{available} \geq E_{consumption}, \\ E_{available} - E_{inv,loss} - E_{dischar,loss}, & \text{if } E_{available} < E_{consumption}. \end{cases} \quad (17)$$

When energy cannot be used to power the load or recharge the battery pack, excess energy is left that is not useable. When production is greater than consumption and the batteries are full or the maximum charging power of the batteries is exceeded, the energy increases as a result of the battery's inability to absorb all transmitted energy. Therefore, it should be addressed in two different contexts. The first situation occurs when there is a surplus of output compared to consumption and the batteries are fully charged. Here, the excess energy is determined using the formula below

$$E_{excess,1} = (E_{PV} + E_{wind}) - (E_{load} + E_{inv,loss}). \quad (18)$$

In the second scenario, even though the batteries are not fully charged and production exceeds consumption, the extra energy is more than the maximum charge power of the battery group ($P_{max,c}$). Here, the excess energy is determined using the formula below

$$E_{excess,2} = E_{excess,1} - P_{max,c} \times 1hr. \quad (19)$$

In this case, the $P_{max,c}$ expression is multiplied by 1 hour to translate the power expression into energy. It was multiplied by 1 hour since the simulations were run at intervals of 1 hour. Unmet energy is computed as follows when the energy generated is less than the energy required by the load

$$E_{unmet} = E_{load} - E_{served}. \quad (20)$$

The battery throughput parameter is the other one that needs to be computed. The energy flowing through a battery group over a period of one year is known as the battery throughput. Before charge losses and before discharge losses, throughput is calculated. It is the variation in the energy level of the battery group. This parameter allows for

the calculation of the battery group life. Throughput is calculated by adding the changes in the battery's energy level after charging and after discharging separately and then dividing the result by two. Due to the throughput calculation requiring the unit energy to be charged and discharged, or computed using the unit energy cycle, it is divided by 2 (charge-discharge):

$$Q_{\text{thrp},+} = \sum E_{\text{charge}}, \quad (21)$$

$$Q_{\text{thrp},-} = \sum E_{\text{discharge}}, \quad (22)$$

$$Q_{\text{thrp}} = \frac{Q_{\text{thrp},+} + Q_{\text{thrp},-}}{2}. \quad (23)$$

Here $Q_{\text{thrp},+}$ is the throughput for charge and $Q_{\text{thrp},-}$ is the throughput for discharge. The battery group life can be determined after this step. The throughput expression of the battery group (Q_{thrp}) was determined using the designed system's charge-discharge cycle. A lifetime throughput (Q_{lifetime}) is also available for each battery. This value, which is listed in the battery catalogue, is one that the battery manufacturer is prepared to provide. The calculation below can be used to determine how long a battery pack will last

$$R_{\text{bat}} = \frac{N_{\text{batt}} Q_{\text{lifetime}}}{Q_{\text{thrp}}}. \quad (24)$$

IV. CONSTRAINTS AND RELIABILITY

Following all of these computations, the reliability parameter, capacity shortage, can be determined. The limits of the optimisation process are represented by the capacity shortage. Constraints, or the reliability parameter, are the requirements that systems must meet. The optimisation method excludes systems that do not adhere to the stated limitations. Operating reserves must be identified before the capacity shortage can be calculated. The operating reserve is the extra operating capacity that can supply energy even during unexpected increases in load or losses in production. In the simulations, the dimensions of the energy-generating components are chosen in such a way as to maintain an operating reserve that is equal to or more than the required reserve. A capacity shortage is said to exist when the operating reserve is insufficient. Depending on the amount of power used and the production of renewable energy, the operation reserve is defined by two factors. It can be summarised in Table III.

The hourly load, the outputs of the renewable energy elements, and the current load at the relevant hour are added, along with the relevant values used in the simulations for each of the three components listed in Table III for the relevant hour. The chosen numerical values were chosen in this manner because the HOMER programme claims to be suitable for most systems. The amount of unmet energy is sufficient to determine the capacity shortage. There will undoubtedly be a capacity constraint if the unmet energy is greater than zero. When the unmet energy is less than zero, there can also be a capacity shortage. Unmet energy only considers feeding the load and excludes whether or not operating reserves are fed. The energy produced and the energy in the battery group may not be able to cover the

operational reserves in situations where the unmet energy is less than zero. As a result, the equation below is used to compute the capacity shortage in these two separate scenarios. In other situations, there is no capacity shortage

$$E_{\text{cs}} = \begin{cases} E_{\text{unmet}} + (E_{\text{wind}_{\text{res}}} + E_{\text{PV}_{\text{res}}} + E_{\text{load}_{\text{res}}}) \times \eta_{\text{inv}} & \text{if } E_{\text{unmet}} > 0, \\ \left(E_{\text{wind}_{\text{res}}} + E_{\text{PV}_{\text{res}}} + E_{\text{load}_{\text{res}}} - \frac{E_{\text{net}}}{\eta_{\text{bat}}} \right) \times \eta_{\text{inv}} & \text{if } E_{\text{unmet}} \leq 0. \end{cases} \quad (25)$$

TABLE III. OPERATING RESERVE COMPONENTS AND PERCENTAGES.

Operating reserve components	Reserved components	Selected values to reserve
Load related part	Hourly load (%)	10
Renewable output related part	Solar power output (%)	25
	Wind power output (%)	50

V. COST FUNCTION FORMULATION

As stated earlier, the cost function used in this study is COE. The generation of COE is shown in the flow chart below (see Fig. 5).

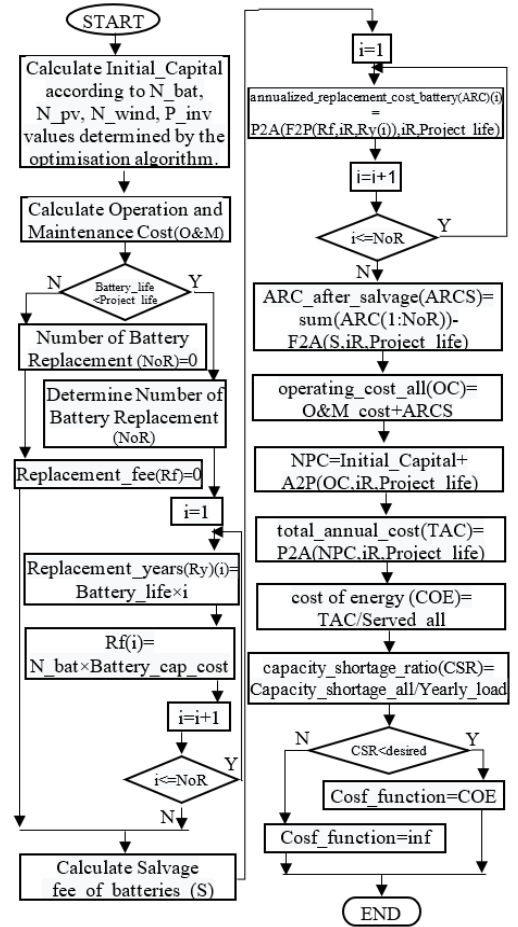


Fig. 5. Economical calculation flow chart.

The initial investment cost is calculated using the number of PV panels (N_{pv}), the number of wind turbines (N_{wind}), the number of batteries (N_{bat}), the power of the inverter (P_{inv}), and the unit costs of these elements at the beginning of the project. The initial investment cost is calculated with the

following equation

$$C_{init} = N_{pv} Cap_{pv} + N_{wind} Cap_{wind} + N_{bat} Cap_{bat} + P_{inv} Cap_{inv}. \quad (26)$$

The cost of operation and maintenance is then determined. The costs of operating and maintaining the component are known as the operating and maintenance cost. The operating and maintenance expenses for each component are determined by dividing the unit cost by the element sizes. The operating and maintenance expenses of each component are then totalled to determine the overall operating and maintenance cost of the system. Costs of operation and maintenance are incurred annually

$$C_{O\&M} = N_{pv} O \& M_{pv} + N_{wind} O \& M_{wind} + N_{bat} O \& M_{bat} + P_{inv} O \& M_{inv}. \quad (27)$$

The number of battery replacements during project life ($R_{proj} = 25$ years) is determined using an uncomplicated mathematical computation after the operating and maintenance costs have been determined

$$N_{rep} = \text{ceil} \left(\frac{R_{proj} - R_{bat}}{R_{bat}} \right). \quad (28)$$

The total replacement cost is computed by taking into account the replacement cost of a battery (Rep_{bat}) after determining how frequently the battery will be replaced and in which years

$$C_{rep} = N_{rep} N_{bat} Rep_{bat}. \quad (29)$$

The remaining life of the batteries and their salvage values should be determined in the event that they do not fully degrade from the year they were last changed until the end of the project life. The following formulas are used to calculate the salvage value and remaining life:

$$R_{rem} = R_{comp} - (R_{proj} - R_{rep}), \quad (30)$$

$$R_{rep} = R_{comp} \text{INT} \left(\frac{R_{proj}}{R_{bat}} \right), \quad (31)$$

$$S = C_{rep} \left(\frac{R_{rem}}{R_{bat}} \right). \quad (32)$$

The salvage value is determined in the right proportion to the remaining battery life under the assumption that the battery depreciation is linear. The annual cost of replacing the batteries should then be computed after this step. The yearly replacement cost is computed by deducting the salvage value at the end of the project life from the total replacement costs spent throughout the project life to get the annual value of the expenditures. Here are the four economic science terms and their short names used in the calculations below. In these formulas, i = interest rate (19 %), n = year, A = annual payment, F = Future value, and P = present value.

Present value of Future value [F2P(F, i, n)]

$$P = \frac{F}{(1+i)^n}. \quad (33)$$

Annual payments of Present value [P2A(P, i, n)]

$$A = \frac{P i (1+i)^n}{(1+i)^n - 1}. \quad (34)$$

Annual payments of Future value [F2A(F, i, n)]

$$A = \frac{F i}{(1+i)^n - 1}. \quad (35)$$

Present value of Annual payments [A2P(A, i, n)]

$$P = \frac{A((1+i)^n - 1)}{i(1+i)^n}. \quad (36)$$

The following equation can be used to determine the annual replacement cost of batteries using the formulas mentioned above

$$C_{arep}(k) = P2A(F2P(C_{rep}(k), i, \text{year}_{rep}(k)), i, R_{proj}). \quad (37)$$

Following the salvage value, the annual replacement cost is as follows

$$C_{arep_after_salvage} = \sum_{j=1}^{N_{rep}} C_{arep}(j) - F2A(S, i, R_{proj}). \quad (38)$$

The annual replacement cost, the annual maintenance and operating cost are combined together to provide the annual operating cost after the salvage value. The total operating cost is the sum of annual replacement cost after salvage value ($C_{arep_after_salvage}$) and annual operating and maintenance costs ($C_{O\&M}$)

$$C_{oper,tot} = C_{O\&M} + C_{arep_after_salvage}. \quad (39)$$

The net present cost of the system is then determined. The expenses incurred over the course of the system's life are included in the net present cost. Investment costs, replacement costs, operating and maintenance costs, and salvage returns are some of these expenses. As a result, the current overall cost of the system is determined as follows

$$C_{NPC} = C_{init} + A2P(C_{oper,tot}, i, R_{proj}). \quad (40)$$

After this step, the total annual cost is calculated as follows

$$C_{ann,tot} = P2A(C_{NPC}, i, R_{proj}). \quad (41)$$

Finally, the energy cost (COE), which acts as a cost function for the DE algorithm, is calculated. The COE is defined as the average cost per kWh of electrical energy served by the system. The COE is calculated as follows

$$COE = \frac{C_{ann,tot}}{\sum_{j=1}^{8760} E_{served}(j)}. \quad (42)$$

The capacity shortage parameter, which is the reliability parameter, is calculated as follows

$$CSR = \frac{\sum_{j=1}^{8760} E_{cs}(j)}{\sum_{j=1}^{8760} E_{load}(j)} \quad (43)$$

The components used in the optimisation, the prices of the components, and other necessary parameters and the selected values are presented in Table IV.

TABLE IV. COMPONENTS AND PARAMETERS.

Parameter	Value
Interest Rate (i)	19 %
Lifetime (n)	25 years
Capacity Shortage	30 %
PV panel price (1 kw)	\$500
PV O&M price (1 kw) (\$/yr)	\$2
Wind Turbine	BWCXL.1
Wind Turbine price (1 kw)	\$1100
WT O&M price (1 kw) (\$/yr)	\$2
Battery	Hoppecke 24 OPzS 3000
Battery Unit Cost	\$660
Bat. O&M price (1 kw) (\$/yr)	\$2
Battery life	10 years

The monthly average meteorological data and load characteristics used in the optimisation are presented in Table V.

TABLE V. SOLAR, WIND, AND LOAD DATA.

Daily Radiation (kWh/m2d)					
Jan	Feb	Mar	Apr	May	Jun
2.012	2.708	4.110	5.300	6.302	6.788
Jul	Aug	Sep	Oct	Nov	Dec
6.812	6.088	4.825	3.371	2.426	1.867
Wind Speed (m/s)					
Jan	Feb	Mar	Apr	May	Jun
8.30	4.80	5.00	3.00	6.25	2.60
Jul	Aug	Sep	Oct	Nov	Dec
10.00	7.37	4.00	6.75	7.75	5.00
Load Characteristics					
Annual average (kWh/d)		Annual average (kWh/hr)		Peak Load (kW)	
7427		309		539	

VI. RESULTS

Three different HRES (PV-WT-BAT-INV), HRES (WT-BAT-INV), and HRES (PV-BAT-INV), with different capacity shortage values, are optimised separately by HOMER and DE algorithm. Optimisation was performed independently using HOMER software and the DE algorithm under the same load and system element conditions. The results of the optimisation of electrical reliability, economy, and computation time were obtained individually and given in Table VI. The search spaces for HOMER and DE can be seen in Table VII.

TABLE VI. COMPARATIVE SIMULATION RESULTS.

HRES TYPE (PV-WT-BAT-INV)						
Economical Results						
	Initial Capital (\$)	Operating Cost (\$/yr)	Total NPC (\$)	Total Annual Capital Cost (\$/yr)	Total O&M Cost (\$/yr)	COE (\$/kWh)
HOMER	1700500	18651	1797395	327325	5500	0.164
DE	1727390	17768	1819700	332500	5686	0.1668
Electrical Results						
	PV Production (kWh/yr)	Wind Production (kWh/yr)	Total Production (kWh/yr)	Served (kWh/yr)	Unmet (KWh/yr)	Excess (kWh/yr)
HOMER	1422371	1837531	3259902	2108154	602691	834111
DE	1423700	1877300	3301000	2100600	610260	887370
	Capacity Shortage (kWh/yr)	Battery Throughput (kWh/yr)	Battery Life (yr)	Battery Autonomy (hr)	Capacity Shortage Ratio (%)	
HOMER	807455	573780	10.70	8.14	30	
DE	820670	548610	10.96	8.0076	30	
	PV Power (kW)	Wind Turbine (Number)	Battery (Number)	Inverter (kW)	Computation Time Results (s)	
HOMER	1100	600	600	450	936	
DE	1101	613	590	539	83	
HRES TYPE (WT-BAT-INV)						
Economical Results						
	Initial Capital (\$)	Operating Cost (\$/yr)	Total NPC (\$)	Total Annual Capital Cost (\$/yr)	Total O&M Cost (\$/yr)	COE (\$/kWh)
HOMER	4044450	12886	4111394	778505	9340	0.346
DE	4106020	9202	4153800	790360	9426	0.348
Electrical Results						
	PV Production (kWh/yr)	Wind Production (kWh/yr)	Total Production (kWh/yr)	Served (kWh/yr)	Unmet (KWh/yr)	Excess (kWh/yr)
HOMER	-----	8498575	8498575	2289686	421167	5885945
DE	-----	8807900	8807900	2294400	417020	6191600
	Capacity Shortage (kWh/yr)	Battery Throughput (kWh/yr)	Battery Life (yr)	Battery Autonomy (hr)	Capacity Shortage Ratio (%)	
HOMER	544491	458146	20	19.92	20	
DE	541480	449050	28.0867	16.7887	20	
	PV Power (kW)	Wind Turbine (Number)	Battery (Number)	Inverter (kW)	Computation Time Results (s)	
HOMER	-----	2775	1320	575	311	
DE	-----	2876	1237	600	28	

HRES TYPE (PV-BAT-INV)						
Economical Results						
	Initial Capital (\$)	Operating Cost (\$/yr)	Total NPC (\$)	Total Annual Capital Cost (\$/yr)	Total O&M Cost (\$/yr)	COE (\$/kWh)
HOMER	4225260	39659	4431293	813309	16172	0.344
DE	4333800	38942	4536100	834190	16563	0.351
Electrical Results						
	PV Production (kWh/yr)	Wind Production (kWh/yr)	Total Production (kWh/yr)	Served (kWh/yr)	Unmet (KWh/yr)	Excess (kWh/yr)
HOMER	6982550	-----	6982550	2479285	231565	4002705
DE	7176600	-----	7176600	2482500	228300	4193500
	Capacity Shortage (kWh/yr)	Battery Throughput (kWh/yr)	Battery Life (yr)	Battery Autonomy (hr)	Capacity Shortage Ratio (%)	
HOMER	273773	1567137	13.9	28.99	10	
DE	270960	1565000	14.2	29.71	10	
	PV Power (kW)	Wind Turbine (Number)	Battery (Number)	Inverter (kW)	Computation Time Results (s)	
HOMER	5400	-----	2136	550	1925	
DE	5550	-----	2189	542	92	

TABLE VII. SEARCH SPACES.

HRES TYPE (PV-WT-BAT-INV)				
	PV	WT	BAT	INV
HOMER	0:50:2000 (41 entries)	0:50:1000 (21 entries)	0:50:1000 (21 entries)	0:50:600 (13 entries)
All different configurations: $41 \times 21 \times 21 \times 13 = 235053$				
DE	0-2000 (inf entries)	0-1000 (inf entries)	0-1000 (inf entries)	0-600 (inf entries)
All different configurations: inf				
HRES TYPE (WT-BAT-INV)				
	PV	WT	BAT	INV
HOMER	(no entries)	0:25:4000 (161 entries)	0:24:1488 (63 entries)	0:25:700 (29 entries)
All different configurations: $161 \times 63 \times 29 = 294147$				
DE	(no entries)	0-4000 (inf entries)	0-1488 (inf entries)	0-700 (inf entries)
All different configurations: inf				
HRES TYPE (PV-BAT-INV)				
	PV	WT	BAT	INV
HOMER	0:100:10000 (101 entries)	(no entries)	0:24:4800 (201 entries)	0:25:700 (29 entries)
All different configurations: $101 \times 201 \times 29 = 588729$				
DE	0-10000 (inf entries)	(no entries)	0-4800 (inf entries)	0-700 (inf entries)
All different configurations: inf				

It was discovered that the two optimisation solutions were nearly identical. However, it can be shown that DE takes much less time to compute than HOMER.

VII. DISCUSSION

In this study, a new method is offered to optimise hybrid renewable energy sources, and the results are compared with those of the HOMER programme. The DE algorithm and the dispatch strategy created produced very successful results in the optimisation of the hybrid system, according to the results. When the results were compared with those of the HOMER commercial hybrid system optimisation tool, it was found that they were nearly identical. The planned dispatch approach allowed for nearly identical results to be attained with HOMER. In this regard, the dispatch technique has been shown to be practical, efficient, and trustworthy.

The search space is established prior to simulation in the HOMER programme. This is actually the most challenging aspect of using HOMER, which makes it a drawback. The search space contains the intended values for each component that will be used in the simulation. HOMER asks

for the search space to be increased if these values are entered insufficiently at the start of the simulation by displaying a search space error. As a result, the search space must be filled with values appropriate for the load or optimum values. Since it will be challenging to foresee the search space while designing huge power systems, the user frequently changes the search space using HOMER's search space error. This makes the optimisation procedure more difficult. Despite the fact that the search space load is built with values appropriate for feeding, there is still the issue of precision. In other words, the values entered are acceptable for the load, however, they might not be exactly tolerable levels. As a result, rather than being sparsely represented by a small number of variables, the search space range should frequently be generated with many values. However, the HOMER will run longer and take longer to produce results the more values are specified. Due to this, it is often necessary to begin with large steps in order to quickly discover the solution before updating the search space again with smaller ones. In other words, a rough optimum is discovered first, and then the precise optimums are sought using these rough optimums as a guide. No matter which optimisation strategy you use, the search space must be large enough to contain the optimum values. The number of states that need to be evaluated and the simulation time would both rise proportionally if values were entered more regularly, lasting hours or even days.

This time the DE algorithm has been used to solve this problem. When using the DE algorithm for optimisation, a search space is not required. To evaluate the element, only the lower and upper values of the value range are entered. The DE algorithm also gave the lower and upper values entered in the HOMER application. However, the DE method does not take into account the values in between. The DE method slices indefinitely between the lower and upper values to determine the ideal value. As a result, the precision and search space error issues are resolved. In addition to these benefits, the key benefit of the DE algorithm is that it can arrive at the result relatively quickly, as seen in Table VI. Metaheuristic algorithms are known to reach the optimum quickly. This study was carried out because of the prediction that the metaheuristic algorithm can reach the solution faster than HOMER. There are studies in the literature showing that metaheuristic algorithms are much faster than HOMER. In the study by

Javed and Ma [5], it is observed that GA is faster than HOMER when the studies in the literature that compare metaheuristic algorithms with HOMER are analysed. This result supports our research. In the study by Ayan and Toyman [20], it was highlighted that the artificial bee colony (ABC) algorithm completes the optimisation much faster than HOMER. Once again, this study supports ours.

If the findings are effectively summarised, it can be said that this work proposes an original dispatch method and a new optimisation tool that combine this dispatch strategy and the DE algorithm to solve HOMER's speed and search space problems. In contrast to the research in the literature, a novel strategy is used to apply this optimisation tool to the optimisation of hybrid renewable energy sources. The reliability parameter employed in the optimisation is LPSP, as can be observed when the studies in the literature are analysed in Table I. In this study, the capacity shortage parameter was used, which has previously mentioned its advantages and advantages over LPSP. The capacity shortage parameter was used for the first time in the optimisation of renewable energy systems with a heuristic algorithm. In previous studies, optimisation was performed with the help of the LPSP reliability parameter, and an advanced dispatch strategy was not recommended. This study closes the gap here. Furthermore, it is clear that earlier research did not incorporate comprehensive computations. For example, research on the charging and discharging of batteries has not been done. However, the charge-discharge rule for batteries is a crucial factor. Battery life, excess energy, unmet energy, served energy, and therefore COE are all significantly impacted by this regulation. Furthermore, previous research did not calculate variables such as battery life, excess energy, unmet energy, and served energy. However, these parameters are crucial parameters that reflect the strengths and weaknesses of the system and provide crucial information about it. Because of this, HOMER determines each of these characteristics.

It has been demonstrated that the method can be used by itself in optimisation procedures when evaluated with HOMER. However, by quickly locating the optimal values with the tool developed in this study, the search space of the HOMER programme can be generated with frequent values near this optimum if working with the commercial software HOMER is required. As a result, the path to the solution is significantly shorter.

VIII. CONCLUSIONS

The goal of this project is to create an optimisation tool that is quicker, more practical, and simpler than HOMER software. The results and corroborating research in the literature indicate that the target goal was achieved. In the future, a tool that can synthesise realistic load, wind speed, and radiation data and then optimise using these can be created. To obtain the vast volume of input-output data needed for deep learning or machine learning optimisation, these techniques can be incorporated into the optimisation procedures.

CONFLICTS OF INTEREST

The author declares that he has no conflicts of interest.

REFERENCES

- [1] R. Storn and K. Price, "Differential evolution - A simple and efficient heuristic for global optimization over continuous spaces", *Journal of Global Optimization*, vol. 11, pp. 341–359, 1997. DOI: 10.1023/A:1008202821328.
- [2] A. Tabak, E. Kayabasi, M. T. Guneser, and M. Ozkaymak, "Grey wolf optimization for optimum sizing and controlling of a PV/WT/BM hybrid energy system considering TNPC, LPSP, and LCOE concepts", *Energy Sources, Part A: Recovery, Utilization, and Environmental Effects*, vol. 44, no. 1, pp. 1508–1528, 2022. DOI: 10.1080/15567036.2019.1668880.
- [3] H. Wei, S. Chen, T. Pan, J. Tao, and M. Zhu, "Capacity configuration optimisation of hybrid renewable energy system using improved grey wolf optimiser", *Int. J. Comput. Appl. Technol.*, vol. 68, no. 1, pp. 1–11, 2022. DOI: 10.1504/IJCAT.2022.123234.
- [4] W. Dong, Y. Li, and J. Xiang, "Optimal sizing of a stand-alone hybrid power system based on battery/hydrogen with an improved Ant Colony Optimization", *Energies*, vol. 9, no. 10, p. 785, 2016. DOI: 10.3390/EN9100785.
- [5] M. S. Javed and T. Ma, "Techno-economic assessment of a hybrid solar-wind-battery system with genetic algorithm", *Energy Procedia*, vol. 158, pp. 6384–6392, 2019. DOI: 10.1016/j.egypro.2019.01.211.
- [6] M. Izdin.Hlal, V. K. Ramachandaramurthy, F. H. Nagi, and T. A. R. Bin Tuan Abdullah, "Optimal techno-economic design of standalone hybrid renewable energy system using genetic algorithm", *IOP Conf. Ser. Earth Environ. Sci.*, vol. 268, no. 1, pp. 1–8, 2019. DOI: 10.1088/1755-1315/268/1/012012.
- [7] M. M. Samy, S. Barakat, and H. S. Ramadan, "A flower pollination optimization algorithm for an off-grid PV-fuel cell hybrid renewable system", *Int. J. Hydrogen Energy*, vol. 44, no. 4, pp. 2141–2152, 2019. DOI: 10.1016/j.ijhydene.2018.05.127.
- [8] A. Fathy, K. Kaaniche, and T. M. Alanazi, "Recent approach based social spider optimizer for optimal sizing of hybrid PV/wind/battery/diesel integrated microgrid in Aljouf region", *IEEE Access*, vol. 8, pp. 57630–57645, 2020. DOI: 10.1109/ACCESS.2020.2982805.
- [9] M. Kharrich *et al.*, "Developed approach based on equilibrium optimizer for optimal design of hybrid PV/wind/diesel/battery microgrid in Dakhla, Morocco", *IEEE Access*, vol. 9, pp. 13655–13670, 2021. DOI: 10.1109/ACCESS.2021.3051573.
- [10] A. S. Al-akayshe, O. N. Kuznetsov, and H. M. Sultan, "Application of Equilibrium Optimization algorithm for optimal design of PV/hydroelectric pumped storage energy system, case study - Iraq", in *Proc. of 2021 IEEE Conf. Russ. Young Res. Electr. Electron. Eng. (ElConRus) 2021*, 2021, pp. 1354–1359. DOI: 10.1109/ElConRus51938.2021.9396604.
- [11] R. Mouachi, M. A. Jallal, F. Gharnati, and M. Raoufi, "Multiobjective sizing of an autonomous hybrid microgrid using a multimodal delayed PSO algorithm: A case study of a fishing village", *Comput. Intell. Neurosci.*, vol. 2020, art. ID 8894094, 2020. DOI: 10.1155/2020/8894094.
- [12] M. Taslimi, P. Ahmadi, M. Ashjaee, and M. A. Rosen, "Design and mixed integer linear programming optimization of a solar/battery based Conex for remote areas and various climate zones", *Sustain. Energy Technol. Assessments*, vol. 45, art. 101104, 2021. DOI: 10.1016/j.seta.2021.101104.
- [13] N. Rahmani and M. Mostefai, "Multi-objective MPSO/GA optimization of an autonomous PV-wind hybrid energy system", *Eng. Technol. Appl. Sci. Res.*, vol. 12, no. 4, pp. 8817–8824, 2022. DOI: 10.48084/etasr.4877.
- [14] G. Bo *et al.*, "Optimum structure of a combined wind/photovoltaic/fuel cell-based on amended Dragon Fly optimization algorithm: A case study", vol. 44, no. 3, pp. 7109–7131, 2022. DOI: 10.1080/15567036.2022.2105453.
- [15] Y.-P. Xu, P. Ouyang, S.-M. Xing, L.-Y. Qi, M. khayatnezhad, and H. Jafari, "Optimal structure design of a PV/FC HRES using amended Water Strider Algorithm", *Energy Reports*, vol. 7, pp. 2057–2067, 2021. DOI: 10.1016/j.egypr.2021.04.016.
- [16] M. Jamshidi and A. Askarzadeh, "Techno-economic analysis and size optimization of an off-grid hybrid photovoltaic, fuel cell and diesel generator system", *Sustain. Cities Soc.*, vol. 44, pp. 310–320, 2019. DOI: 10.1016/j.scs.2018.10.021.
- [17] K. Lee and D. Kum, "Complete design space exploration of isolated hybrid renewable energy system via dynamic programming", *Energy Convers. Manag.*, vol. 196, pp. 920–934, 2019. DOI: 10.1016/j.enconman.2019.05.078.
- [18] H. A. El-Sattar, S. Kamel, M. H. Hassan, and F. Jurado, "Optimal sizing of an off-grid hybrid photovoltaic/biomass gasifier/battery

system using a quantum model of Runge Kutta algorithm”, *Energy Convers. Manag.*, vol. 258, art. 115539, 2022. DOI: 10.1016/j.enconman.2022.115539.

- [19] A. Maleki and A. Askarzadeh, “Artificial bee swarm optimization for optimum sizing of a stand-alone PV/WT/FC hybrid system considering LPSP concept”, *Sol. Energy*, vol. 107, pp. 227–235, 2014. DOI: 10.1016/j.solener.2014.05.016.
- [20] S. Ayan and H. Toylan, “Size optimization of a stand-alone hybrid photovoltaic/wind/battery renewable energy system using a heuristic optimization algorithm”, *Int. J. Energy Res.*, vol. 46, no. 11, pp. 14908–14925, 2022. DOI: 10.1002/er.8192.
- [21] T. Tezer, R. Yaman, and G. Yaman, “Evaluation of approaches used for optimization of stand-alone hybrid renewable energy systems”, *Renew. Sustain. Energy Rev.*, vol. 73, pp. 840–853, 2017. DOI: 10.1016/j.rser.2017.01.118.
- [22] J. F. Manwell and J. G. McGowan, “Lead acid battery storage model for hybrid energy systems”, *Sol. Energy*, vol. 50, no. 5, pp. 399–405, 1993. DOI: 10.1016/0038-092X(93)90060-2.



This article is an open access article distributed under the terms and conditions of the Creative Commons Attribution 4.0 (CC BY 4.0) license (<http://creativecommons.org/licenses/by/4.0/>).